CrossMark

Research Article

Using pH Gradient Dissolution with *In-Situ* Flux Measurement to Evaluate Bioavailability and DDI for Formulated Poorly Soluble Drug Products

Jane Li,[1] Konstantin Tsinman,[2,3] Oksana Tsinman,[2] and Larry Wigman[1]

ABSTRACT. This study described a pH-gradient dissolution method combined with flux measurements as an *in vitro* tool for assessing the risk of bioavailability reduction due to drug-drug interactions (DDI) caused by acid reducing agents (ARAs). The device incorporates absorption chambers into USP II dissolution vessels, with fiber optic UV-probes monitoring concentration *in situ*. Dosage forms of Genentech BCS class II drugs, GDC-0810, GDC-0941, and compound A, were tested by starting the dissolution in either pH 1.6 or pH 4.0 media then converting to FaSSIF after 30 min. GDC-0810 showed no significant difference in flux between the two conversion experiments. A supersaturation phase was observed for GDC-0941 in the pH 1.6 experiments after media conversion to FaSSIF; however, it did not appear to occur in the pH 4.0 experiment due to low drug solubility at pH 4.0, resulting in a 95% decrease in flux compared to pH 1.6 experiment. The extent of flux reduction and the total accumulated API mass in the absorption chamber agreed well with the 89% reduction in mean Cmax and the 82% reduction in mean AUC from dog PK study between animals treated with pentagastrin and famotidine. Testing of the compound A optimized formulation tablets showed a 25% reduction in flux and *in vitro* absorbed amount by changing pH 1.6 to 4.0, correlating well with the AUC decrease in clinical studies. Good correlation between *in vitro* data and *in vivo* PK data demonstrated the applicability of the method for formulators to develop drug products mitigating DDI from ARAs.

KEY WORDS: pH gradient dissolution; *in-situ* flux measurement; acid reducing agents (ARAs); drug-drug interactions (DDIs); dosage form.

INTRODUCTION

Developing formulations to effectively deliver poorly soluble new drugs during early clinical phases is especially challenging due to the moving targets of tolerability and efficacy with limited clinical pharmacokinetic (PK) data. The challenge continues to grow with estimates of 40 to 70% of new drugs entering development characterized as poorly soluble (1). Animal models and modeling software have been widely employed to predict the *in vivo* performance of drug formulations (2–4); yet, each has limited prediction power for complex formulations designed to maintain a supersaturated state for poorly soluble drugs (5–7). Dogs are the most common species for preclinical PK studies; however, they have different gastrointestinal (GI)

physiology compared to humans, with gastric pH being most significant and impactful (8). Therefore, animal studies often require pre-medication of each animal to adjust stomach pH to more human-like conditions (4,9–10).

Tsume *et al*. (5) proposed subclasses of acid (a), base (b), and neutral (c) for BCS class II to study mechanistically the *in vitro/in vivo* behavior of the poorly soluble drugs. Acidic BCS class IIa drugs have very low solubility under normal gastric pH conditions and are dissolved and absorbed later in the intestine where the pH is higher. The solubility of neutral BCS class IIc compounds does not depend on pH. Thus, variation in gastric pH has minimal impact on their bioavailability. The basic BCS class IIb drugs are readily solubilized under low gastric pH conditions and must remain in solution to be absorbed in the proximal portion of the intestine (*e.g*., duodenium and jejunum) (4,5). As the result, the bioavailability of these drugs is expected to be highly dependent on gastric pH and is particularly challenging for patients with hypochlorhydria or patients taking acid reducing agents (ARAs). ARAs are widely prescribed to treat various disorders related to gastroesophageal hyperacidity (11). It

Guest Editor: Sandra Klein

[1] Genentech, South San Francisco, California 94080, USA.
[2] Pion Inc., 10 Cook St, Billerica, Massachusetts 01821, USA.
[3] To whom correspondence should be addressed. (e–mail: ktsinman@pion-inc.com)

aaps

has been reported that up to 50% of cancer patients take ARAs, with some cancer populations, such as GI and pancreatic having even greater use of ARAs (12). Since ARAs increase the gastric pH, their use can consequentially and detrimentally affect the exposure of BCS IIb drugs, resulting in large decrease in bioavailability due to drug-drug interactions (DDIs) (13–15).

Various formulation approaches have been assessed for BCS class IIb drugs to enhance the bioavailability and overcome the potential DDIs with ARAs (6,7,10,16). For example, to mitigate the problem of reduced absorption of weak base BMS-561389, formulations containing organic acids, sulfobutylether-β-cyclodextrin or povidone were developed and showed enhanced dissolution, and gastric pH had no impact on drug absorption in the canine model for tablets containing tartaric acid (16). Mitra et al. (10) explored several formulations for the development of a weakly basic, BCS class IIb oncology compound to overcome the achlorhydria effect, including the addition of the acidifier in the formulation, enhanced formulations via hot melt extrusion with copovidone and/or citric acid, stabilized nanosuspensions, and alternative drug salt form.

To enhance the efficiency of formulation development, in vitro dissolution and predictive models have been developed as powerful tools to screen drug formulations and predict their in vivo behavior (17). Dissolution testing in Biorelevant media with or without pH gradient was shown to be useful in characterizing solid dosage forms of poorly water soluble drugs and establishing in vitro-in vivo correlation (IVIVC) (18–22); however, this single-phase dissolution approach had little consideration of the drug absorption process and may not reliably predict the in vivo dissolution and release of these drugs. Biphasic dissolution methods utilize an aqueous phase where drug dissolution occurs under non-sink condition and an immiscible organic phase into which the dissolved drug partitions under sink condition (23–26). Because the amount of drug partitioned into the organic phase is dictated by the free drug concentration in the aqueous phase, the organic phase behaves like an "absorption chamber" and allows the assessment of the in vivo dissolution-absorption processes. The biphasic dissolution approach has been demonstrated to be flexible for characterizing various dosage forms and suitable for IVIVC. Main drawbacks of the biphasic dissolution experiments include difficulty in sampling from the two phases and the use of big quantities of an organic solvent (such as octanol) that can be unpleasant or hazardous.

To overcome these experimental challenges, systems that combine dissolution and absorption chambers were introduced to study various factors influencing drug absorption (27–30). The membrane separating dissolution and absorption chambers include a cell-based monolayer, such as Caco-2 (27,28), a regenerated cellulose size exclusion membrane (29), and an artificial lipophilic membrane as commonly used in parallel artificial membrane permeability assay (PAMPA) (30). PAMPA membrane was first introduced by Kansy et al. (31) for high-throughput permeability screening of the discovery compounds and widely accepted for permeability measurements due to the good correlation with Caco-2 cultures and rat perfusion models (32,33). The approach of in vitro dissolution with permeability was reported for prediction of systemic exposure of BCS class II drug

clarithromycin (34) and quantitative prediction of pH-dependent DDIs with ARAs (30). In the first study (34), clarithromycin formulations were tested with in vitro dissolution and dissolution/permeation across two types of membranes; comparison with in vivo data from rats showed strong correlation using Caco-2 membrane but not with the excised rat intestinal sheets. For the DDIs study, Zhu et al. (30) developed a novel two-stage in vitro dissolution-permeation (IVDP) system that combines micro-dissolution concept and PAMPA membrane to mimic drug absorption. The in vitro pH-dependent DDI data collected for 11 weakly basic compounds with known clinical pH-dependent DDI data suggest that the in vitro data could be used to predict the extent of the clinical pH-dependent DDI. Despite the promising results, the IVDP as reported could not be used to assess the actual solid dosage forms because of the small volume of the chambers and the media. Borbás et al. (35) just published a study using IVDP based on a standard USP II apparatus to compare final dosage forms of brand name and generic versions of telmisartan. The data from the study demonstrated the applicability of such device for assessing the risks of bioequivalence failure.

The goal of this paper was to study the DDIs with ARAs of three Genentech drugs using IVDP. For the purpose of this study, DDI refers to the pH solubility/dissolution-based DDIs only. Final dosage forms of each drug were tested for dissolution and permeation in media simulating both normal and hypochlorhydric gastric conditions followed by pH gradient to FaSSIF conditions. A BCS class IIa drug, GDC-0810, was selected as a model compound for which DDI with ARAs was not expected. Other drugs were BCS Class IIb with in vivo data available. The first one, GDC-0941, exhibited significant DDI with ARAs in vivo (9). The second drug, compound A, had significant DDI with ARAs that was largely overcome by formulation with acidic excipients (22). The in vitro data were compared to in vivo results for correlation and to evaluate the feasibility of USP II based IVDP as a predictive tool for DDI of BCS class II compounds with ARAs.

MATERIALS AND METHODS

Solid dosage forms of the three Genentech proprietary compounds, formulated for immediate release, were prepared by Genentech (South San Francisco, CA) for this study. Table I summarizes the physicochemical properties of each active pharmaceutical ingredient (API) and the relevant information of the drug product. GDC-0810 is a monoprotic acid, developed as a meglumine salt, and formulated as a tablet containing 200 mg of GDC-0810 as free acid. GDC-0941 is a diprotic base, developed as a dimethylate salt, and formulated as a tablet containing 20 mg of GDC-0941 as free base. Compound A is a triprotic base, developed as free base, and formulated as a tablet containing 50 mg of API.

Simulated intestinal fluid (SIF) powder was purchased from Biorelevant (biorelevant.com). All other reagents were purchase from Sigma-Aldrich (St. Louis, MO) unless otherwise stated and were HPLC grade or better.

Flux measurements were performed using MacroFLUX™ apparatus (Pion Inc., Billerica MA, USA) shown in Fig. 1.

Table I. API Physicochemical Properties and Relevant Formulation Information

API/BCS class	Functional formulation additive	Strength (mg)	MW	pKa[1]	logP[2]	Solubility in pH 1.0	Solubility in FaSSIF
GDC-0810 Meglumine salt BCS IIa	Sodium bicarbonate	200	446.90 (free acid); 642.11 (salt)	4.3	6.2	0.1 µg/mL	3.18 mg/mL
GDC-0941 Dimethylate salt BCS IIb	None	20	513.64 (free base); 705.84 (salt)	1.6; 4.3	2.1	0.75 mg/mL	<1 µg/mL
Compound A Free base BCS IIb	Fumaric acid	50	664.81	1.1; 3.3; 5.0	3.3	>100 mg/mL	~1 µg/mL

[1] Measured values using acid-base titrations
[2] Measured values using shake-flask measurements

In this IVDP device, four cylindrical absorption chambers were inserted into modified vessel covers of the dissolution bath (Model DT 126 Light, Erweka Heusenstamm, Germany). For each experiment, the dissolution (donor) vessels were filled with 800 ml of either pH 1.6 buffer that simulated unmodified simulated gastric fluid (SGF) or pH 4.0 buffer simulating alkalized simulated gastric fluid (ASGF). The volume for the gastric media was selected to result in 1000 mL of FaSSIF after the conversion (see Table II and related conversion protocol below). The final volume ensured that the absorption chamber was submerged to the FaSSIF dissolution medium. Any drug permeation that was happening during SGF or ASGF stage was minimal and ignored because stomach related absorption was believed to be negligible for the studied compounds. The donor vessels were separated from the absorption (receiver) chambers by a horizontally positioned filter supported membrane. Prior to the assay, the membrane was formed by placing 50 µL of 20% lecithin in dodecane lipid solution (GIT Lipid, Pion Inc., Billerica MA) on the filter support material (PVDF, polyvinylidenfluoride, 3.88-cm^2 open area, 0.45-µm pore size, 120-µm thickness, 70% nominal porosity). Each receiver chamber contained 12 ml of acceptor sink buffer (ASB, Pion, Inc.). The ASB is a HEPES based pH 7.4 buffer containing

chemical scavengers (surfactants micelles) that maintain sink conditions during the experiments. The compositions of both the membrane and the receiver solution were identical to the Double-Sink™ PAMPA model described elsewhere (32,33).

The experiment began by placing tablets in SGF or ASGF media. After 30 min, media of the donor vessels were converted to 1000 mL of FaSSIF by adding a corresponding concentrate. Table II shows constituents of the concentrates to convert SGF and ASGF to FaSSIF. The composition of the resulting FaSSIF medium was similar to FaSSIF V1 described in the literature (18).

The ratio for the conversion of SGF to FaSSIF was 8:1:1 of corresponding solutions A:B:C from Table II. To prepare ASGF medium, an aliquot of the solution B was added to an aliquot of solution A using ratio 1:11.4, resulting in a solution with pH 4.0 ± 0.2. Conversion from ASGF to FaSSIF was performed based on the ratio of 8:0.3:1 for ASGF:B:C to keep the composition of FaSSIF same for both types of experiments. The pH of the FaSSIF medium was measured immediately after conversion from SGF or ASGF and was confirmed to be 6.5 ± 0.1.

Stirring in the absorption chamber was provided by an overhead stirrer rotating at 450 rpm bundled with measuring mini UV-Vis probe with 1-cm pathlength, and the standard
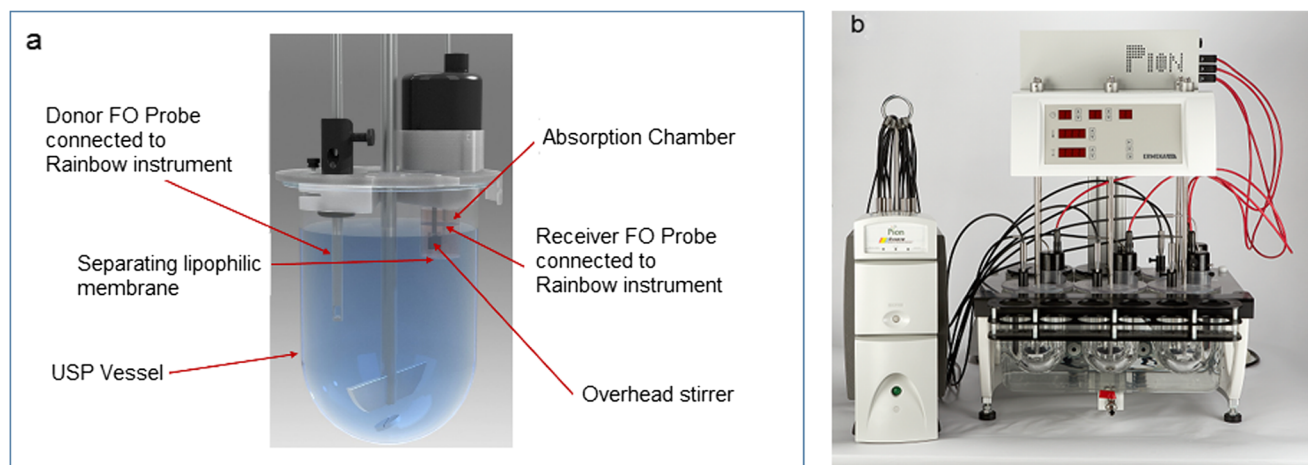
Fig. 1. **a** A schematic showing of dissolution–absorption setup used in this study. **b** A picture of MacroFLUX apparatus showing the dissolution bath, the Rainbow detection system, and four absorption chamber inserts

Table II. Composition of Solutions Used to Convert SGF and ASGF to FaSSIF Media

Reagent	Quantity (units)
SGF (solution A)	
1-N HCl	30.00 (mL)
NaCl	4.50 (g)
Water, qs	1000 (mL)
Phosphate concentrate (solution B)	
NaH$_2$PO$_4$	3.95 (g)
NaCl	1.25 (g)
NaOH pallets	1.34 (g)
Water, qs	100 (mL)
Lecithin concentrate (solution C)	
SIF powder	2.240 (g)
Water, qs	100 (mL)

paddle of USP II apparatus provided stirring at 100 rpm in the dissolution vessels. Rotating speed in the absorption chamber was selected to ensure homogeneity of the solution for the concentration measurements. Media in dissolution vessel and absorption chamber were maintained at 37 ± 0.5°C.

The UV signals of the samples in all four dissolution vessels and absorption chambers were monitored *in situ* using fiber optic (FO) UV-Vis probes connected to the Rainbow® instrument (Pion Inc., Billerica, MA, USA). The standard solutions of all compounds were prepared using serial addition method. For each compound, a stock solution was prepared by dissolving the API powder in MeOH at a concentration within ~ 5–10 mg/mL range. The FO probes were positioned in a beaker containing 40–50 mL of the preheated corresponding medium. Calculated aliquots of the stock solution were then added and spectral data were obtained for at least six concentrations, ensuring proper mixing of the stock solution with the media occurred prior to the measurements. Care was taken to make sure no precipitations occurred during the standard preparations. Table III below summarizes the details of the standard preparation and analytical parameters used for *in situ* concentration monitoring.

The standard calibration curves were built using the area under the second derivative curve within the wavelength ranges specified in Table III. These ranges were identified to minimize the influence of spectral noise on the data. The second derivative spectroscopy was used to correct for scatter effects in the donor chambers. Linearity of the standard curves was characterized by $r^2 > 0.999$. Drug concentrations in the donor and receiver chambers were then calculated using the UV absorbance and the corresponding standard curves. The pH of the donor chamber solution was checked after the measurements and was 6.5 ± 0.2 for all experiments. Concentration-time profiles were monitored over at least 300 min, in triplicate for each formulation. Flux (J) was calculated from the obtained concentration-time profiles for the receiver chambers. Flux is the measurement of the mass transfer through the membrane and is defined as total amount of material (or mass) crossing one unit area of the membrane per unit time, as provided by Eq. (1):

$$J = \frac{dm}{A \cdot dt} = \frac{V}{A} \cdot \frac{dc}{dt} \qquad (1)$$

where A is the area of the membrane (3.88 cm^2), V is the volume of the absorption chamber, and $\frac{dc}{dt}$ ($\mu g \cdot ml^{-1} \cdot min^{-1}$) is the slope of the concentration-time profile of corresponding API in the absorption chamber. In this study the "early" (initial) and the "late" (final) flux values were calculated by fitting the concentration-time profile in the absorption chambers to the straight line, followed by normalization to volume and area ratio according to Eq. (1). Time intervals were selected based on the apparent linearity of the concentration-time profiles. The linear portions of the curves were fitted ensuring that lag time was excluded. It has to be noted that time intervals for fitting had to be selected differently for some formulations reflecting their particular kinetics.

RESULTS

Dissolution and concentration profile of GDC-0810 are shown in Fig. 2a, b. The first 30 min of dissolution measurements was performed in either SGF or ASGF media

Table III. Summary of Standard Preparations and Parameters for Sample Analysis

Compound	Medium	Standard curve range, μg/mL	Pathlength, mm	Analytical range, nm (second derivative absorbance)
GDC-0810	SGF	4–200	2	356–382
	ASGF	4–200	2	300–326
	FaSSIF	6–200	2	294–320
	ASB	20–200	10	368–384
GDC-0941	SGF	4–20	10	350–370
	ASGF	4–20	10	350–370
	FaSSIF	4–20	10	350–370
	ASB	4–20	10	350–370
Compound A	SGF	10–50	5	308–326
	ASGF	10–50	5	300–326
	FaSSIF	10–50	5	308–326
	ASB	10–50	10	386–400

after which it was converted to FaSSIF. The disintegration of the tablets occurred during SGF/ASGF stage as expected for the immediate release products. The flux was calculated using Eq. (1) (Table IV) and presented in Fig. 2c together with total amount of GDC-0810 accumulated in the receiver chamber after 240 min in Fig. 2d. The time intervals of 60–100 and 240–300 min were used for linear fit of concentration-time profile in the absorption chamber and to calculate the "early" and the "late" flux correspondingly for this compound.

Results for compounds GDC-0941 and compound A are presented in Figs. 3 and 4. Experiment conditions were same as those described in the "MATERIALS AND METHODS" section. Panels a and b in Figs. 3 and 4 are the dissolution and concentration profiles of GDC-0941 and Compound A, respectively. The flux and the total amount of the accumulated API in the receiver chamber after 240 min were calculated (Table IV) and presented in Figs. 3c–d and 4c–d, respectively, for the two compounds.

DISCUSSION

Gastric pH is known to greatly influence the PKs and bioavailability of the poorly soluble small molecule drugs, especially the BCS class IIb compounds. Therefore, variations on individual gastric pH due to hypochlorhydria need to be closely monitored when taking these drugs in order to achieve

optimal medical benefits. Similarly, co-medication of BCS class II drugs with ARAs presents specific development challenges for formulation development and clinical trials because of DDI concerns. Compared to costly and time-consuming animal and human PK studies, *in vitro* methods are preferred in predicting the DDI potential and mitigating the development risks. Indeed, numerous *in vitro* approaches have been reported to predict *in vivo* behavior of oral dosage forms and help guide the formulation development. However, these *in vitro* tools either lacked the ability to take into account the influence of formulations on the absorption step (20,22) or were not designed to work with final dosage forms (28,30). The IVDP used in this study was evaluated to overcome these limitations.

BCS class IIa compound GDC-0810 was selected for this study as a "negative control" as no DDI due to ARAs was expected for this class of drugs. The pH-solubility profile of GDC-0810 as reported previously (36) is shown in Fig. 5a with the solubility < 0.1 μg/mL at pH 1.6 and pH 4.0. However, for the pH gradient experiments at both pH 1.6 and 4.0, GDC-0810 drug product reached at least 60% dissolved and the API concentration greater than 150 μg/mL (Fig. 2b). This concentration was remarkably higher than expected solubility of free acid API at corresponding pH values (Fig. 5a). Such kinetic behavior could be attributed to the microenvironmental pH modulation of GDC-0810 tablet
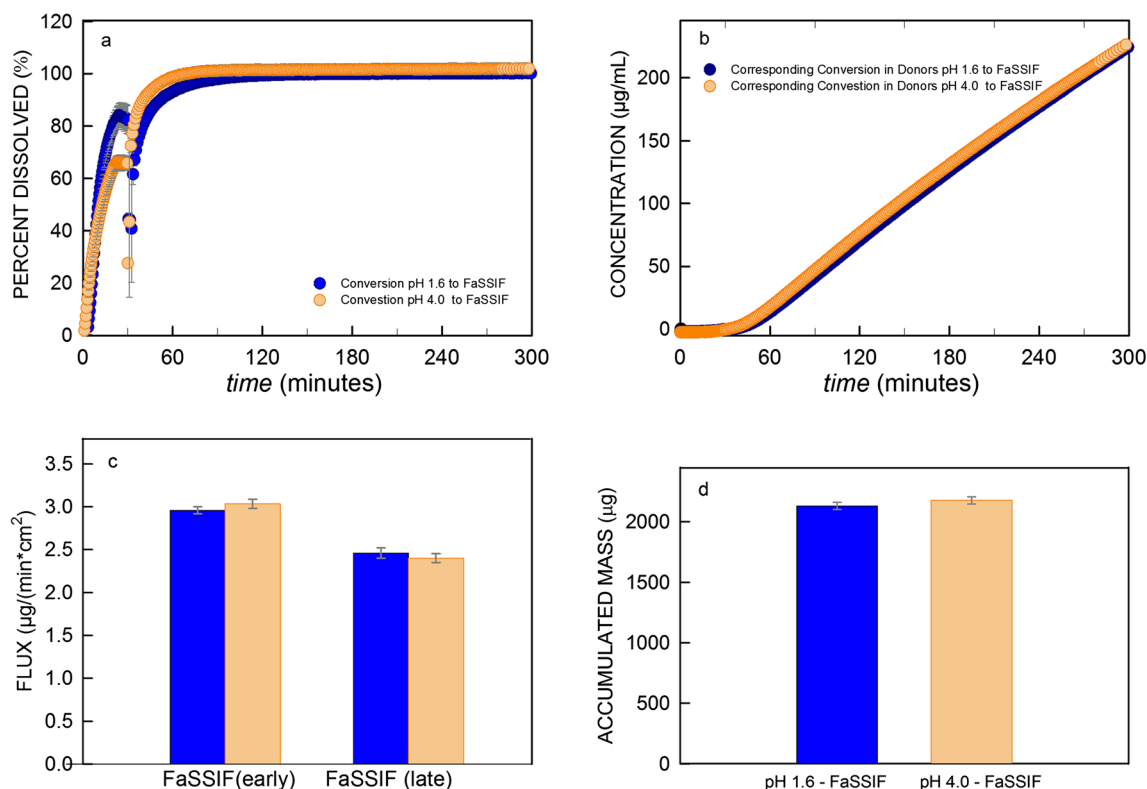
Fig. 2. Dissolution and flux results for GDC-0810 (average of four replicates). The first 30 min corresponds to the SGF or ASGF media followed by conversion to FaSSIF. Blue and orange dots represent SGF→FaSSIF and ASGF→FaSSIF pH gradient experiments, respectively. **a** Profile of percent dissolved (%D) *versus* time in the dissolution vessels. **b** Profile of concentration *versus* time in the absorption chambers. **c** Flux values calculated based on Eq. (1) and using linear fit of concentration-time profile in the receiver for 60–120 min ("early) and 240–300 min ("late"). **d** Total amount of the drug in the receiver chamber after 240 min of the experiment. The standard deviations in the dissolution vessels for 40–300 min interval (**a**) and in the absorption chamber for 0–300-min interval (**b**) did not exceed ± 2.3% and ± 3.6 μg/mL correspondingly; thus, error bars could not be noticed on the graphs

Table IV. Summary of Flux and Accumulated Mass of API in Absorption Chamber at 240 min[a]

| Parameter		GDC-0810		GDC-0941		Compound A	
		pH 1.6	pH 4.0	pH 1.6	pH 4.0	pH 1.6	pH 4.0
Flux ($\mu g \cdot min^{-1} \cdot cm^{-2}$)	FaSSIF (early)	2.959 (0.042)	3.037 (0.054)	0.410 (0.068)	0.020 (0.005)	0.724 (0.043)	0.537 (0.006)
	FaSSIF (late)	2.460 (0.059)	2.402 (0.049)	0.127 (0.020)	0.024 (0.003)	0.480 (0.015)	0.430 (0.027)
Accumulated mass at 240 min (μg)		2129.7 (30.4)	2175.9 (29.8)	232.0 (21.5)	18.0 (4.1)	503.2 (26.0)	379.8 (4.6)

[a] All results were calculated and reported as mean based on triplicate measurements in SGF → FaSSIF experiments and four replicate measurements in ASGF → FaSSIF experiments. Standard deviation (SD) was in parentheses

formulation incorporating sodium bicarbonate (36). Following the insignificant difference between dissolution in SGF and ASGF media, the compound reached the complete dissolution in FaSSIF within 20 min of conversion for both cases (Fig. 2a), showing identical flux and the accumulated total mass in the receiver chambers regardless of SGF or ASGF media (Fig. 2c and d). Thus, based on the flux experiments, no DDI risk from ARAs would be expected, agreeing with the assessment based on the properties of this BCS IIa compound. Some reduction in flux for this compound at later time could be attributed to the loss of sink conditions in the receiver chambers as the concentration there exceeded those in the corresponding donor vessels.

Both GDC-0941 and Compound A are BCS class IIb compounds. GDC-0941 is a weak diprotic base with the pK_a of 1.6 and 4.3 and the pH-solubility profile (Fig. 5b) that had previously been reported (9).

As evident from Fig. 5b, the solubility of GDC-0941 would decrease almost 2 orders of magnitude if pH of the stomach increased from pH ~ 1.6 to pH 4.0, thus significant DDI with ARAs would be expected. Indeed, as shown in Fig. 3, a drastic decrease in absorbed amount of GDI-0941
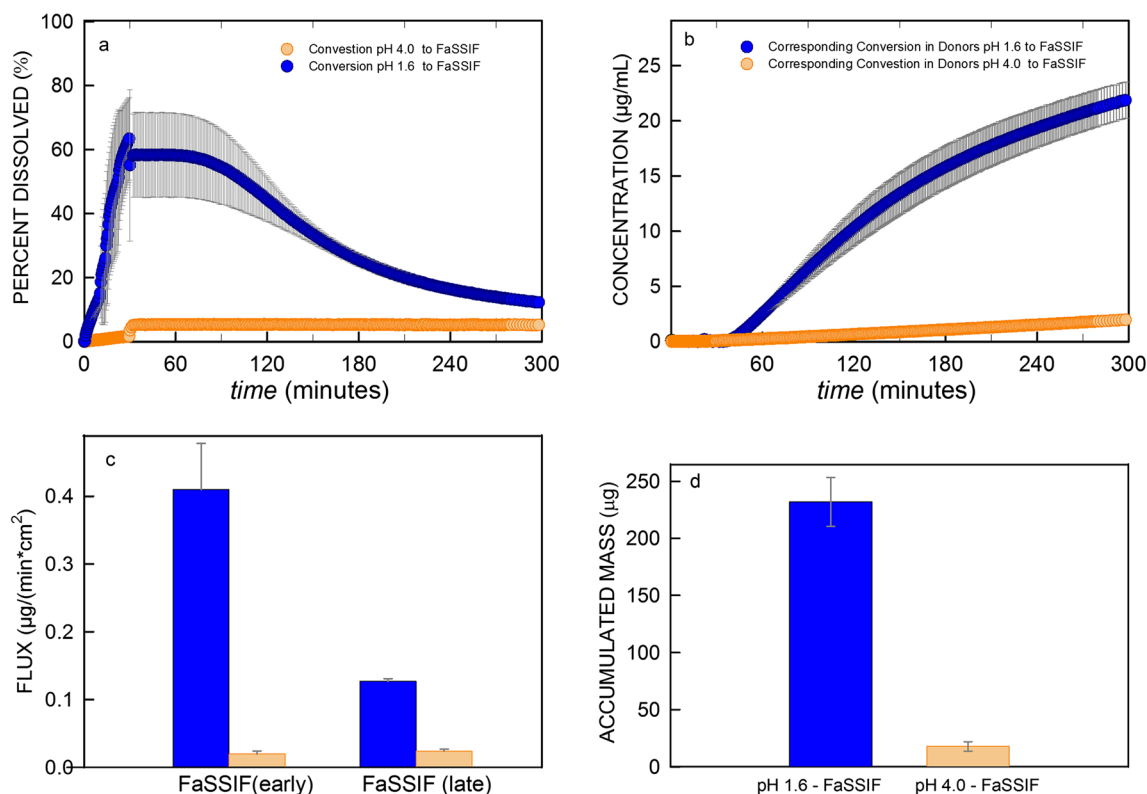
Fig. 3. Dissolution and flux results for GDC-0941 (average of four replicates). The first 30 min corresponds to the SGF or ASGF media followed by conversion to FaSSIF. Blue and orange dots represent SGF → FaSSIF and ASGF → FaSSIF pH gradient experiments, respectively. **a** Profile of percent dissolved (%D) *versus* time in the dissolution vessels. **b** Profile of concentration *versus* time in the absorption chambers. **c** Flux values calculated based on Eq. (1) and using linear fit of concentration-time profile in the receiver for 60–120 min ("early) and 240–300 min ("late"). **d** Total amount of the drug in the receiver chamber after 240 min of the experiment. The standard deviations in the dissolution vessels (**a**) did not exceed 2.2% for SGF → FaSSIF gradient within 120–300-min interval and 0.6% for ASGF → FaSSIF gradient within the entire duration of the experiment, respectively. The standard deviations in the absorption chamber in case of ASGF → FaSSIF gradient were below 0.5 μg/mL. The error bars representing such SD values could not be seen on the corresponding graphs
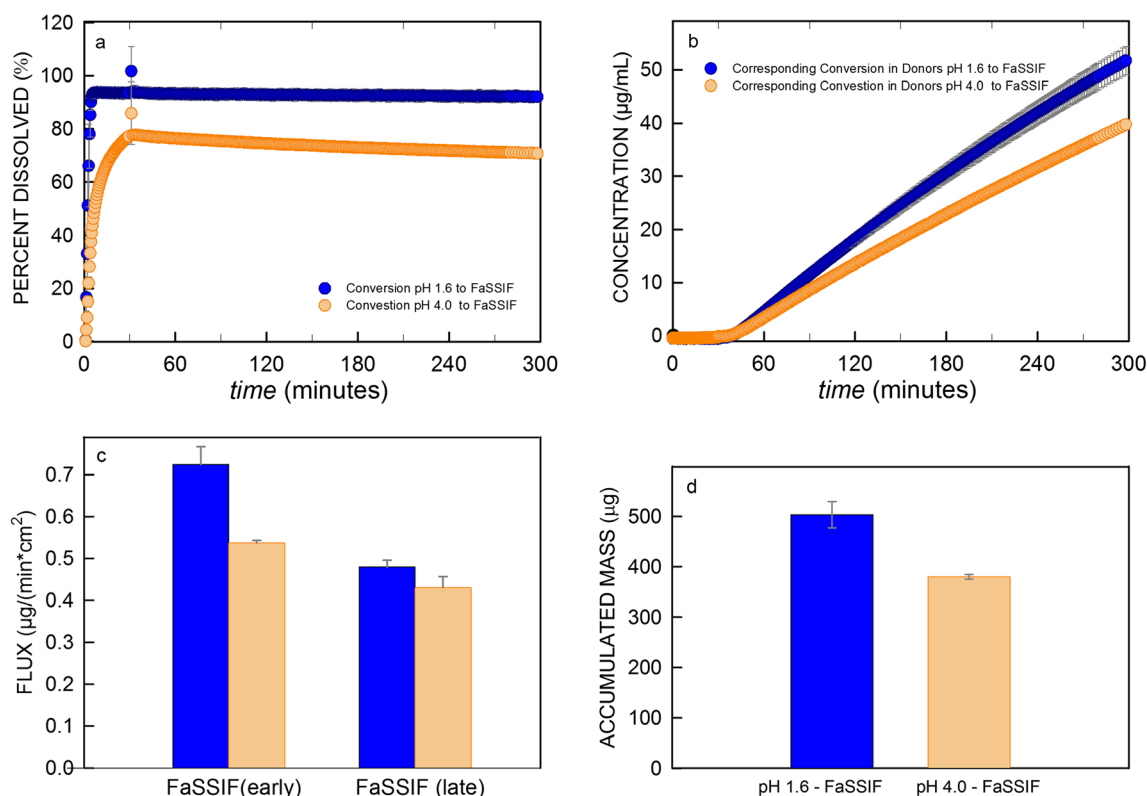
Fig. 4. Dissolution and flux results for Compound A (average of four replicates). The first 30 min corresponds to the SGF or ASGF media followed by conversion to FaSSIF. Blue and orange dots represent SGF→FaSSIF and ASGF→FaSSIF pH gradient experiments, respectively. **a** Profile of percent dissolved (%D) *versus* time in the dissolution vessels. **b** Profile of concentration *versus* time in the absorption chambers. **c** Flux values calculated based on Eq. (1) and using linear fit of concentration-time profile in the receiver for 60–120 min ("early") and 240–300 min ("late"). **d** Total amount of the drug in the receiver chamber after 240 min of the experiment. Within 40–300-min interval the standard deviations in the dissolution vessels (**a**) did not exceed 2.6% for SGF→FaSSIF gradient and 1.0% for ASGF→FaSSIF gradient, respectively. The standard deviations in the absorption chamber in case of ASGF→FaSSIF gradient were below 0.5 μg/mL. The error bars representing such SD values could not be seen on the corresponding graphs

was confirmed by the dissolution-flux measurements. GDC-0941 was observed to dissolve approximately 60% in experiments started with SGF and remained dissolved for approximately 90 min after medium conversion to FaSSIF (Fig. 3a). The difference between its solubility at pH 6.5 (Fig. 5b) and the measured maximum concentration in FaSSIF (Fig. 3a) indicated that the compound remained supersaturated during this period of time. The flux of API was 0.41 $\mu g \cdot mL^{-1} \cdot cm^{-2}$ during the initial supersaturating phase. After 90 min, GDC-0941 slowly precipitated in the dissolution vessel (Fig. 3a) with flux in the receiver/absorption chamber reducing 70% to 0.127 $\mu g \cdot mL^{-1} \cdot cm^{-2}$ (Fig. 3c). Such reduction in flux corresponded well with the drop of the concentration in the donor compartment (Fig. 3a) and thus was likely to be attributed to the precipitation of GDC-0941 in donor rather than to the loss of the sink conditions in the absorption chamber. In contrast, in the ASGF assay, only approximately 2% of GDC-0941 was dissolved with no supersaturation phase after conversion to FaSSIF in the dissolution vessel (Fig. 3a). Flux in the absorption chamber was practically unchanged (Fig. 3b, c) at ~ 0.02 $\mu g \cdot mL^{-1} \cdot cm^{-2}$ after conversion to FaSSIF, a decrease of 95% compared to the flux in SGF assay during the supersaturation phase. The total accumulated amount of API at 240 min reduced approximately 92% (Fig. 3d) from 232 μg in SGF → FaSSIF

conversion to 18 μg in ASGF → FaSSIF conversion. As illustrated in Fig. 6a, the extent of reduction in flux and the total accumulated API mass in the absorption chamber agreed well with the 89% reduction in mean C_{max} and the 82% reduction in mean AUC that were measured in dog PK study between animals treated with pentagastrin and famotidine (9), demonstrating the potential of the method as a predictive tool for assessing DDI with ARAs. The results also shed light on formulation strategy for a challenging molecule such as GDC-0941. In order to have sufficient drug available *in vivo* even under elevated gastric pH conditions, the formulation would need to incorporate excipient(s) to help solubilize and maintain the solubilization of the drug under these conditions.

Compound A is a triprotic base with pK_a of 1.1, 3.3, and 5.0. Its pH-solubility profile (Fig. 5c) looks very similar to GDC-0941. DDI with ARAs was reasonably expected to become a major risk if not addressed properly and was indeed confirmed by animal and human PK studies (22). Unlike GDC-0941, tablets of compound A with optimized formulations (Table I) were tested in this study. The formulation optimization was to overcome the issue of reduced bioavailability triggered by DDI with ARAs or elevated gastric pH due to hypochlorhydria. As shown in Fig. 4a, Compound A quickly reached almost full dissolution in SGF and was about
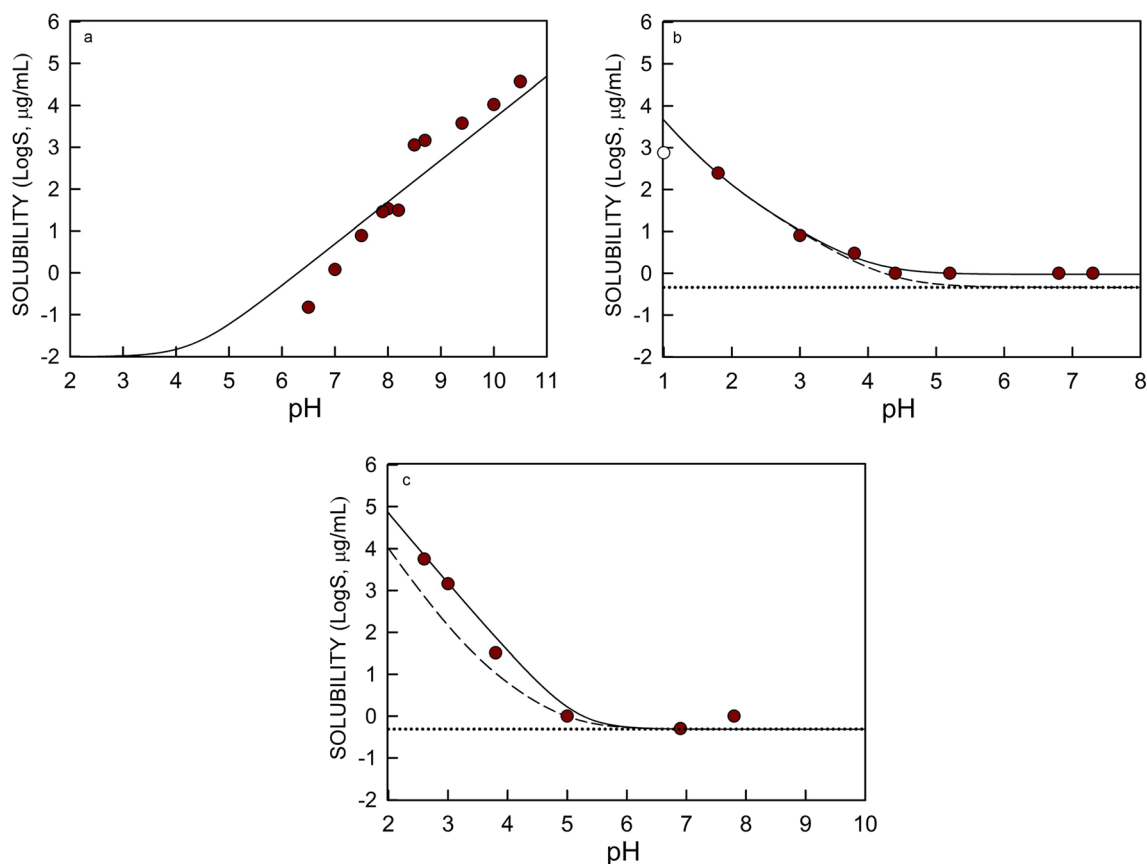
Fig. 5. Solubility–pH profile for GDC-0810 (**a**), GDC-0941 (**b**), and Compound A (**c**). The solid line was the best fit to the modified Henderson-Hasselbalch (HH) equation taking into account potential aggregation phenomena (37). Dashed line represented unmodified HH fit taking into account pK$_a$ values from Table I. Dotted line showed intrinsic solubility limit. For GDC-0810, there was a poor fit to both modified and classical HH models and thus there was no separation between solid and dashed lines

80% dissolved after 30 min in ASGF. After the media conversion to FaSSIF, the compound remained well dissolved for the duration of both experiments, strongly suggesting supersaturation of the drug in the FaSSIF media. In addition, the difference in %dissolved did not significantly change during the supersaturation state for both converted FaSSIF media, and some reduction in "late" flux might be attributed to the loss of the sink conditions in the absorption chamber. The initial flux in the absorption chamber for ASGF → FaSSIF conversion experiment was about 75% of the value for SGF → FaSSIF conversion. Same ratio was obtained when comparing the total accumulated mass of the
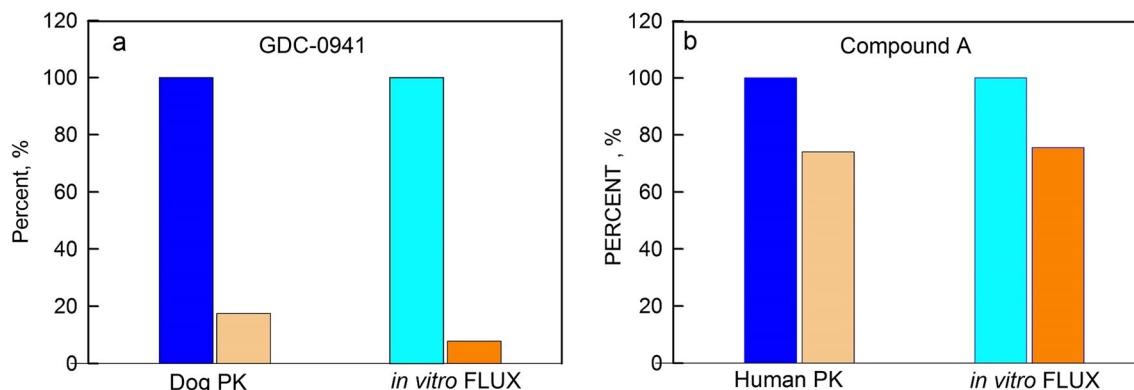
Fig. 6. Plot of %reduction of *in vivo* AUC compared to %reduction of *in vitro* flux values under "hypochlorhydric" *vs.* normal gastric pH conditions for GDC-0941 (**a**) and compound A (**b**). *In vivo* (dark blue) and *in vitro* (light blue) responses under normal gastric pH conditions were designated as 100%; *in vivo* (light brown) and *in vitro* (orange) responses under hypochlorhydric gastric pH conditions were normalized against the corresponding responses under normal gastric pH conditions

API in the receiver chamber at 240 min for the ASGF assay (380 μg) with the total mass for the SGF assay (503 μg). The ratios for flux and the total accumulated mass from this pH gradient study agree remarkably well with the ratio of AUC_{0-24} from the human PK studies, which was measured to be 0.74 for subjects taking these tablets with *vs.* without rabeprazole pretreatment (22). These results were presented in Fig. 6b and again demonstrated the potential of the method as a predictive tool for pharmaceutical development, strongly suggesting that the USP II based IVDP device employed for this study could be valuable for formulation development of the challenging BCS Class IIb compounds.

Finally, it was observed that the accumulated mass at 240 min was only about 1–1.5% of the total dose studied (Table IV). The small amount of total dose absorbed was primarily due to the relatively small membrane area available for the transport in the MacroFLUX device and the limited volume of the absorption chamber. It is hypothesized that, by considering 240 min to be a characteristic small-intestine transit time, the amount of *in vitro* absorbed drug could correlate with the mass of absorbed drug *in vivo*. The exploration of this hypothesis, though, is within the scope of future research. For the current studies, instead of directly comparing the accumulated mass *in vitro* to the amount of absorbed drug *in vivo*, the ratio of *in vitro* results (total accumulated mass and flux) was compared to the ratio of *in vivo* C_{max} or AUC. This has been shown to be an acceptable approach in demonstrating the potential of this USP II based IVDP as a predictive tool for DDI of BCS class II compounds with ARAs and for pharmaceutical development.

CONCLUSIONS

This study tested final clinical dosage forms of three drugs using a USP II based *in vitro* dissolution-permeation device. The obtained dissolution and flux results were in good correlation with dog and human PK data for the two BCS class IIb compounds, while no *in vivo* study was conducted for the BCS class IIa compound GDC-0810 based on scientific rationale. This study demonstrated that the IVDP combining absorption chamber with the USP II dissolution apparatus was well suited for testing the final dosage forms directly, and the method of pH gradient dissolution combined with absorption step could be used as *in vitro* predictive tool for evaluating the DDI risks from ARAs for BCS Class IIb drugs and expediting formulation development efforts in mitigating such risks. This approach is currently being explored for other BCS class II compounds at Genentech to further assess its applicability and limitations.

ACKNOWLEDGEMENTS

REFERENCES

1. Elder DP. Effective formulation development strategies for poorly soluble active pharmaceutical ingredients (APIs). Am Pharm Rev. 2011;12(2):56–61.
2. Lignet F, Sherbetjian E, Kratochwil N, Jones R, Suenderhauf C, Otteneder MB, *et al*. Parrott N characterization of pharmacokinetics in the Gottingen minipig with reference human drugs: an in vitro and in vivo approach. Pharm Res. 2016;33:2565–79.
3. Zhang T, Heimbach T, Lin W, Zhang J, He HD. Prospective predictions of human pharmaceutics for eighteen compounds. J Pharm Sci. 2015;104:2795–806.
4. Bhattachar SN, Perkins EJ, Tan JS, Burns LJ. Effect of gastric pH on the pharmacokinetics of a BCS class II compound in dogs: utilization of an artificial stomach and duodenum dissolution model and GastroPlus™ simulations to predict absorption. J Pharm Sci. 2011;100:4756–65.
5. Tsume Y, Mudie DM, Langguth P, Amidon GE, Amidon GL. The biopharmaceutics classification system: subclasses for in vivo predictive dissolution (IPD) methodology and IVIVC. Eur J Pharm Sci. 2014;57:152–63.
6. Lainé AL, Price D, Davis J, Roberts D, Hudson R, Back K, *et al*. Enhanced oral delivery of celecoxib via the development of a supersaturable amorphous formulation utilizing mesoporous silica and co-loaded HPMCAS. In J Pharm. 2016;512:118–25.
7. Van Speybroeck M, Mols R, Mellaerts Randy R, Thi TD, Martens JA, Van Humbeeck J, *et al*. Combined use of ordered mesoporous silica and precipitation inhibitors for improved oral absorption of the poorly soluble weak base itraconazole. Eur J Pharm Biopharm. 2010;75:354–65.
8. Lui CY, Amidon GL, Berardi RR, Fleisher D, Youngberg C, Dressman JB. Comparison of gastrointestinal pH in dogs and humans: implications on the use of the beagle dogs as a model for oral absorption in humans. J Pharm Sci. 1986;75:271–4.
9. Pang J, Dalziel G, Dean B, Ware JA, Salphati L. Pharmacokinetics and absorption of the anticancer agents dasatinib and GDC-0941 under various gastric conditions in dogs—reversing the effect of elevated gastric pH with betaine HCl. Mol Pharm. 2013;10:4024–31.
10. Mitra A, Kesisoglou F, Beauchamp M, Zhu W, Chiti F, Wu Y. Using absorption simulation and gastric pH modulated dog model for formulation development to overcome achlorhydria effect. Mol Pharm. 2011;8:2216–23.
11. Targownik LE, Metge C, Roos L, Leung S. The prevalence of and the clinical and demographic characteristics associated with high-intensity proton pump inhibitor use. Am J Gastroenterol. 2007;102:942–50.
12. Smelick GS, Heffron TO, Chu L, Dean B, West DA, DuVall SL, *et al*. Prevalence of acid-reducing agents (ARAs) in cancer patients and ARA drug-drug interaction potential for molecular targeted agents in clinical development. Mol Pharm. 2013;10:4055–62.
13. Koneru B, Cowart DT, Noorisa M, Kisicki J, Bramer SL. Effect of increasing gastric pH with famotidine on absorption and oral pharmacokinetics of the inotropic agent vesnarinone. J Clin Pharmacol. 1998;38:429–32.
14. Budha NR, Frymoyer A, Smelick GS, Jin JY, Yago MR, Dresser MJ, *et al*. Drug absorption interactions between oral targeted anticancer agents & PPIs: is pH-dependent solubility the achilles heel of targeted therapy? Clin Pharmacol Ther. 2012;92:203–13.
15. Lahner E, Annibale B, Fave GD. Systemic review: impaired drug absorption related to the co-administration of antisecretory therapy. Aliment Pharmacol Ther. 2009;29:1219–29.
16. Badawy SIF, Gray DB, Zhao F, Sun DX, Schuster AE, Hussain MA. Formulation of solid dosage forms to overcome gastric pH interaction of factor Xa inhibitor, BMS-561389. Pharm Res. 2006;23:989–96.
17. Kostewicz ES, Abrahamsson B, Brewster M, Brouwers J, Butler J, Carlert C, *et al*. In vitro models for the prediction of in vivo performance of oral dosage forms. Eur J Pharm Sci. 2014;57:342–66.

18. Klein S. The use of Biorelevant dissolution media to forecast the in vivo performance of a drug. AAPS J. 2010;12:397–406.

19. Klein S, Dressman JB. Comparison of drug release from metoprolol modified released forms in single buffer versus a pH-gradient dissolution test. Dissolution Technologies. 2006;13:6–11.

20. Mathias NR, Xu Y, Patel D, Grass M, Caldwell B, Jager C, et al. Assessing the risk of pH-dependent absorption for new molecular entities: a novel in vitro dissolution test, physicochemical analysis and risk assessment strategy. Mol Pharm. 2013;10:4063–73.

21. Gao P, Shi Y. Characterization of supersaturatable formulations for improved absorption of poorly soluble drugs. AAPS J. 2012;14:703–13.

22. Kou D, Dwaraknath S, Fischer Y, Nguyen D, Kim M, Yiu H, et al. Biorelevant dissolution models for a weak base to facilitate formulation development and overcome reduced bioavailability caused by hypochlorhydria or achlorhydria. Mol Pharm. 2017;10:3577–87.

23. Pestieau A, Evrard B. In vitro biphasic dissolution tests and their suitability for establishing in vitro-in vivo correlations: a historical review. Eur J Pharm Sci. 2017;102:203–19.

24. Xu H, Shi Y, Vela S, Marroum P, Gao P. Developing quantitative in vitro-in vivo correlation for fenofibrate immediate-release formulations with the biphasic dissolution–partition test method. J Pharm Sci. 2018;107:476–87.

25. Heigoldt U, Sommer F, Daniels R, Wagner K-G. Predicting in vivo absorption behavior of oral modified release dosage forms containing pH-dependent poorly soluble drugs using a novel pH-adjusted biphasic in vitro dissolution test. Eur J Pharm Biopharm. 2010;75:105–11.

26. Deng J, Staufenbiel S, Bodmeier R. Evaluating a biphasic in vitro dissolution test for estimating the bioavailability of carbamazepine polymorphic forms. Eur J Pharm Sci. 2017;105:64–70.

27. Kataoka M, Masaoka Y, Sakuma S, Yamashita S. Effect of food intake on the oral absorption of poorly water-soluble drugs: in vitro assessment of drug dissolution and permeation assay system. J Pharm Sci. 2006;95(9):2051–61.

28. Kataoka M, Fukahori M, Ikemura A, Kubota A, Higashino H, Sakuma S, et al. Effects of gastric pH on oral drug absorption: in vitro assessment using a dissolution/permeation system

reflecting the gastric dissolution process. Eur J Pharm Biopharm. 2016;101:103–11.

29. Raina SA, Zhang GGZ, Alonzo DE, Wu J, Zhu D, Catron ND, et al. Enhancements and limits in drug membrane transport using supersaturated solutions of poorly water soluble drugs. J Pharm Sci. 2014;103(9):2736–48.

30. Zhu A, Ho MC, Gemski CK, Chuang BC, Liao M, Xia C. Utilizing in vitro dissolution-permeation chamber for the quantitative predication of pH-dependent drug-drug interactions with acid-reducing agents: a comparison with physiologically based pharmacokinetic modeling. AAPS J. 2016;18:1512–23.

31. Kansy M, Senner F, Gubernator K. Physicochemical high throughput screening: parallel artificial membrane permeation assay in the description of passive absorption processes. J Med Chem. 1998;41:1007–10.

32. Avdeef A, Artursson P, Neuhoff S, Lazorova L, Grasjoe J, Tavelin S. Caco-2 permeability of weakly basic drugs predicted with the double-sink PAMPA pKfluxa method. Eur J Pharm Sci. 2005;24:333–49.

33. Bermejo M, Avdeef A, Ruiz A, Nalda R, Ruell JA, Tsinman O, et al. PAMPA—a drug absorption in vitro model 7. Comparing rat in situ, Caco-2, and PAMPA permeability of fluoroquinolones. Eur J Pharm Sci. 2004;21:429–41.

34. Forner K, Holm R, Morakul B, Junyaprasert VB, Ackermann M, Mazur J, et al. Dissolution and dissolution/permeation experiments for predicting systemic exposure following oral administration of the BCS class II drug clarithromycin. Eur J Pharm Sci. 2017;101:211–9.

35. Borbás E, Nagy ZK, Nagy B, Balogh A, Farkas B, Tsinman O, et al. The effect of formulation additives on in vitro dissolution-absorption profile and in vivo bioavailability of telmisartan from brand and generic formulations. Eur J Pharm Sci. 2018;114(January):310–7. Available from: http://linkinghub.elsevier.com/retrieve/pii/S0928098717306954

36. Hou HH, Jia W, Liu L, Cheeti S, Li J, Nauka E, et al. Effect of microenvironmental pH modulation on the dissolution rate and oral absorption of the salt of a weak acid—case study of GDC-0810. Pharm Res. 2018;35(2):37. https://doi.org/10.1007/s11095-018-2347-z.

37. Avdeef A, Bendels S, Tsinman O, Tsinman K, Kansy M. Solubility-excipient classification gradient maps. Pharm Res. 2007;24(3):530–45.